



HAL
open science

Transition kinetics of mixed lipid:photosurfactant assemblies studied by time-resolved small angle X-ray scattering

J. Royes, V.A. Bjørnstad, G. Brun, T. Narayanan, R. Lund, Christophe C. Tribet

► To cite this version:

J. Royes, V.A. Bjørnstad, G. Brun, T. Narayanan, R. Lund, et al.. Transition kinetics of mixed lipid:photosurfactant assemblies studied by time-resolved small angle X-ray scattering. *Journal of Colloid and Interface Science*, 2022, 610, pp.830-841. 10.1016/j.jcis.2021.11.133 . hal-03526492

HAL Id: hal-03526492

<https://hal.science/hal-03526492>

Submitted on 19 Apr 2022

HAL is a multi-disciplinary open access archive for the deposit and dissemination of scientific research documents, whether they are published or not. The documents may come from teaching and research institutions in France or abroad, or from public or private research centers.

L'archive ouverte pluridisciplinaire **HAL**, est destinée au dépôt et à la diffusion de documents scientifiques de niveau recherche, publiés ou non, émanant des établissements d'enseignement et de recherche français ou étrangers, des laboratoires publics ou privés.

Transition kinetics of mixed lipid:photosurfactant assemblies studied by time-resolved Small Angle X-ray Scattering

J. Royes,¹ V.A.Bjørnstad,² G. Brun,¹ T. Narayanan³, R. Lund,² C. Tribet¹

¹. PASTEUR, Département de chimie, École normale supérieure, PSL University, Sorbonne Université, CNRS, 75005 Paris, France

². Department of Chemistry, University of Oslo, P.O. Box 1033, Blindern, N-0315 Oslo, Norway

³. ESRF-The European Synchrotron, 71 Avenue des Martyrs, F-38043 Grenoble, France

Abstract:

Hypothesis. Photoswitchable surfactants are used in the design of many light-responsive colloids and/or self-assemblies. Photo-isomerization enables to control molecular equilibrium, and triggers transient reorganizations with possibly out-of-equilibrium intermediate states that have been overlooked. Here, we address this question by an *in depth* structural investigation of intermediate lipid-surfactant assemblies that occur during fast isothermal photo-triggered transition in lipid:surfactant mixtures.

Experiments. The structural parameters of mixed assemblies of azobenzene-containing cationic surfactant (AzoTMA) and dioleoylphosphatidylcholine (DOPC) lipids were studied by light scattering and time-resolved small angle X-ray scattering. Structural and compositional information about the assemblies and unimers in bulk were determined at the photostationary states, as well as at intermediate kinetic states formed during UV or blue light illumination.

Findings. DOPC:AzoTMA systems form mixed assemblies representative of phospholipid:cationic surfactant mixtures, that evolve from spheroid, to rod-like micelles, and vesicles with increasing DOPC fraction. Transient assemblies detected during the photo-triggered kinetics are similar to the ones found in stationary states. But changes of AzoTMA unimers in bulk can be considerably faster than mass reorganizations of the mixed assemblies, suggesting that out-of-equilibrium conditions are transiently reached. Mass reorganization of the surfactant-enriched assemblies is much faster than in the lipid enriched ones, providing insight into the role of lipids in a slow reorganization of the assemblies.

Keywords

Azobenzene , cationic surfactants, photoswitch, vesicles, micelles, kinetics, TR-SAXS

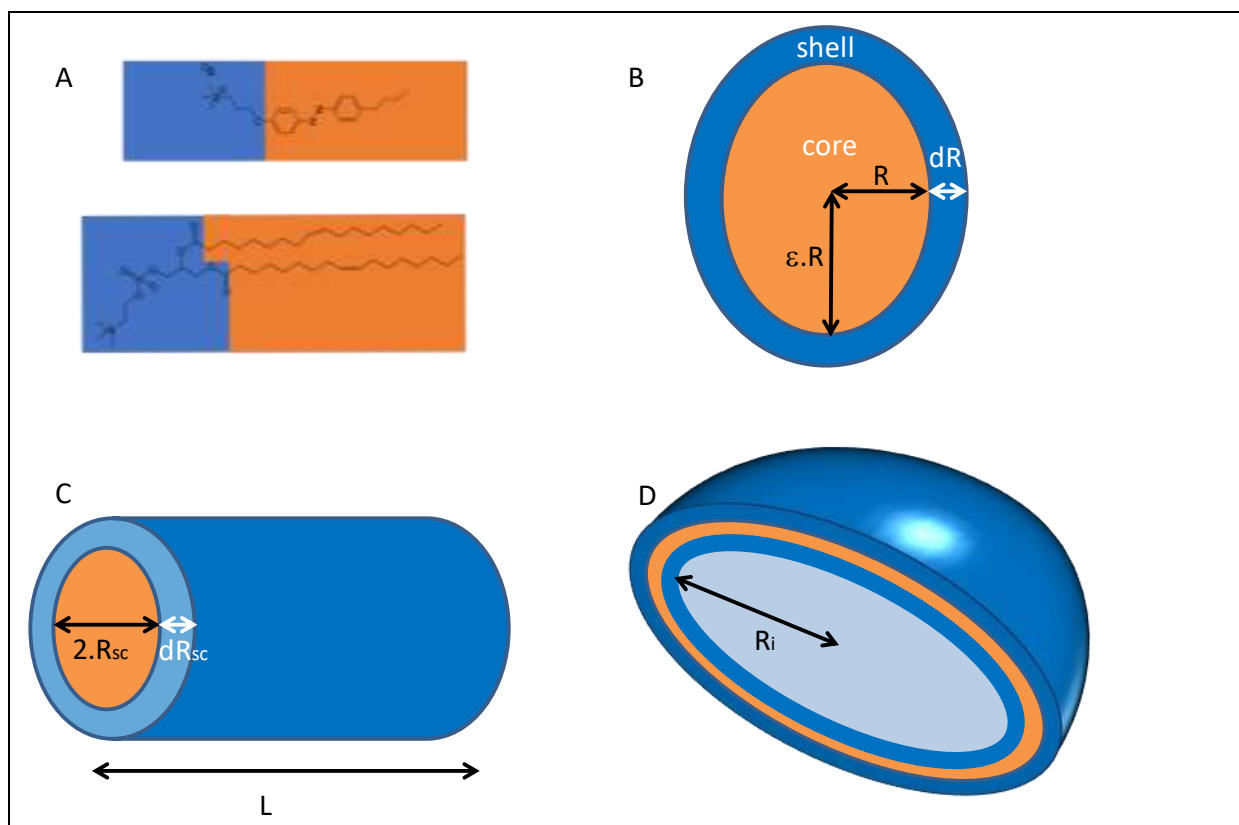
Introduction

Reviews on switchable surfactants [1],[2],[3],[4] regularly update a seemingly endless variety of applications that are accomplished by remote control on the molecular assemblies of amphiphiles, both in bulk and/or at interfaces. Light-responsive amphiphilic systems provide contactless control and high spatial and temporal resolution, which have been exploited in applications such as additive-free modulations of properties (eg. interfacial motion [3], triggered gelation [5],[6]), wetting/dewetting [7], emulsion stability and stability of foams [8, 9], encapsulation/release by micelles or vesicles [10]). Because of their robustness and synthetic versatility, azobenzene-containing photosurfactants are predominant molecular players in the field [3, 4],[11]. The *trans*-to-*cis* photoisomerization of azobenzene moieties modifies both the hydrophobicity and the molecular geometry of the surfactant, which in turn can trigger mesoscopic reorganizations in amphiphilic assemblies that propagate up to macroscopic changes. In fact, different illumination conditions produce differences in the photostationary *cis:trans* ratio, enabling impressive variations in the macroscopic properties. However, fast kinetics of the mesoscopic and macroscopic structural transitions between photostationary states of assemblies of azobenzene surfactants have rarely been investigated. Representative structural studies of photokinetics in solutions of azo-surfactants were typically obtained with non-laser sources, resulting in variation in (self)assemblies during several seconds up to hours (recorded with sampling of the order of seconds or minutes time scales [12],[13, 14]). Of note, the time scales involved in the dynamic self-assemblies of single-tail surfactants are generally very short (e.g. <ms for micellization). Using non-laser light sources the photo isomerization is generally much slower than the adsorption/desorption rates at interfaces [15], micellization [16] or formation of rod-like micelles [14]. Accordingly, the few available kinetics studies cited above probed structural evolutions that were rate-limited by photoisomerization of the surfactant. When the isomerization rate controls assemblies, the observed intermediate structures correspond to equilibrium assemblies achieved at each instantaneous molecular compositions (including at varying ratio between *cis* and *trans* isomers). This raises the question of whether possible out-of-equilibrium intermediate steps may have been overlooked at shorter time scales. Interestingly, limitation by photoisomerization rate may not necessarily result in quasi-equilibrium situations. Near interfaces or more generally when diffusive motion can occur at long-enough time scales, illumination of photo-switchable molecules together with diffusion-controlled binding/associations, are basic ingredients of out-of-equilibrium steady-state regimes resulting in spatial gradients of composition [4]. For instance, uneven exposure to light of interfaces establishes source- and sink-like areas (*i.e.* production:destruction patterns of photoisomers), that "feeds" diffusive motions occurring on a similar time-scale as the light-triggered isomerization. Near-interfacial micrometer-long gradients in water have been rationalized and experimentally assessed at air-water interfaces [17]. One visible consequence of such gradients is the phototactic motion of colloid particles (the term diffusioosmosis was coined by Santer et al. [3],[18]) at an illuminated water-glass interface.

It is still an open question whether non-equilibrium pathways may similarly affect long-living assemblies, such as lipid vesicles in the presence of photoswitchable amphiphiles. Due to their poor solubility, double-tail amphiphiles such as lipids undergo slow molecular exchange with the solution. The characteristics of those systems (size, shape of vesicles and leaflet asymmetry, *etc.*) depend on the preparation and handling protocols, and non-equilibrium states may persist for hours or even days. Optical stimulation of photoactive phospholipids, in which one or both of the acyl chains were functionalized with a photochrome group, creates transient stress in lipid vesicles that are not immediately relaxed by molecular rearrangements or diffusion processes, and may trigger transient pores in the bilayer (see review by [10]). A variety of photosensitive amphiphiles have been used to achieve photoporation of lipid bilayers, such as

azobenzene-modified phospholipids [19, 20], photoswitchable cholesterol [21], spiropyran functionalized lipids [22], diacetylene polymers [23] or azo-peptides [24]). On the other hand, shape curvature or tension of the membrane are other responses to stress that typically occurs in giant unilamellar vesicles (GUV) with *ad hoc* formulations and exposure to light. For instance, artificial lipids with an azobenzene moiety in their headgroup [25], or in their hydrophobic tail [26] and photoswitchable cholesterol [27] have been shown to trigger buddings [25] or markedly affect lipid membrane stiffness [26], fluidity [28, 29], and inhomogeneities (presence or absence of lipid rafts [30]). Recently, dispersions of lipid GUV were doped with water-soluble single tail azo-amphiphiles added in solution. Depending on the composition of the system, exposure to light triggers budding [31], bursting [32] or on demand membrane fusion [33]. The most common hypothesis to explain those results is an abrupt change in the membrane tension upon desorption or adsorption of azo-amphiphiles caused by photoisomerization [33]. However, this assumption of non-equilibrium dynamics of lipids and azo-amphiphiles mixed membranes has not been validated experimentally. Other effects may also be significant, such a disturbance in the hydrophobic core of the membranes due a variation of polarity upon *cis-trans* isomerization. Indeed, change on polarity upon photoisomerization lowers the activation barrier of hemifusion between mixed bilayers containing azobenzene surfactants [34]). In this regard, exploring in detail morphological changes of light-responsive lipid assemblies at the length scales of the bilayer thickness can address the possible existence of out-of-equilibrium intermediates. Time-resolved (TR)-SAXS is a structural method capable of reaching millisecond time scale as well as nanoscale spatial resolution [35]. Furthermore, it has been implemented to study the kinetics of amphiphilic polymer assemblies [36], surfactants [37],[38],[39] and photosurfactant micellization [16]. Fast solubilization of liposomes or spontaneous vesiculation triggered by dilution and/or fast supplementation with detergents have also been investigated by (TR)-SAXS.[40],[41],[42],[43]

In this study we propose to assess for the first time the photo-triggered kinetic pathway of fast light-induced reorganization of mixed assemblies of lipid (DOPC) and azobenzene-containing cationic surfactant (AzoTMA). Using (TR)-SAXS and dynamic light scattering, we addressed the question of whether or not intermediate structures that are formed during the light-stimulated transitions differ from the assemblies formed at photostationary states or in the dark. We studied a range of lipid:azosurfactant compositions either at equilibrium, or exposed to continuous light irradiation, or undergoing the photoswitch of *cis:trans* isomerization of AzoTMA that induced transitions between small micelles (radius of a few nanometers), large vesicles , or elongated rod-like micelles (> 60 nm). In order to get insight into the detailed shape and nanostructure, analytical scattering models developed for the different structures were fitted to the SAXS data (Scheme 1).



Scheme 1. Models of the mixed AzoTMA:DOPC assemblies showing the characteristic structural parameters used to fit SAXS profiles. A) AzoTMA and DOPC chemical structure with head- and tailgroup marked in blue and orange respectively, B) cross-section of a ellipsoidal micelle, C) rod-like micelle, D) spherical vesicle (with interlayer layer thicknesses in blue and orange color corresponding to inner/outer headgroup region and tailgroup region respectively)

Materials and Methods

Preparation of the samples

Two different preparation of lipid:azosurfactant mixtures were used. To assess the solubilisation efficiency of AzoTMA on DOPC bilayers, we added the surfactant in suspensions of pre-made liposomes prepared by hydration of dried DOPC films, whereas to study equilibrium self-assemblies concentrated dispersion of lipids in AzoTMA surfactants were diluted in water. Solvents and buffers were from Sigma-Aldrich, except if specified. AzoTMA was synthesized as described in [16].

Namely, pre-made liposomes were obtained as follows. 0.2 mL of 50 g/L DOPC (Avanti Polar Lipids, USA) in 99%+ $\text{CHCl}_3/\text{MeOH}$ (90:10) was dried at room temperature under nitrogen in HPLC glass flask (ChromacolTM, Thermo Scientific) then under vacuum for 2 h. The film was hydrated in 1 mL water for 2 hours, bath sonicated for 10 minutes and applied three freeze-thaw cycles (liquid nitrogen) / 40°C to reduce the multilamellarity of the formed vesicles. Extrusion through a PVDF 0.22 μm (Millipore) filter, and centrifugation (for 10 minutes at 14,000 g) yielded *ca.* 1 g/L vesicles in water. The liposomes were diluted in water, and mixed at time zero with aliquots of 20 g/L AzoTMA in water to reach the concentration of 0.1g/L DOPC. For the addition of predominantly *cis* isomers of AzoTMA, the 20 g/L stock solution of surfactant was exposed to UV light (7 $\text{mW}\cdot\text{cm}^{-2}$, 365 nm) for 3 hours prior to mixing, and the mixed solutions were incubated under UV light (0.2 $\text{mW}\cdot\text{cm}^{-2}$) overnight.

On the other hand, to prepare mixed AzoTMA:DOPC assemblies, solutions were prepared by hydration of dry DOPC lipid films in concentrated AzoTMA. Solutions containing 0.1 mL of 10 g/L DOPC in CHCl₃/MeOH (90:10) were dried under slow-flowing nitrogen gas at room temperature in a HPLC glass flask and then kept under vacuum for 2 hours. Aliquots of a stock solution of 25 g/L AzoTMA in water (from 200 μL down to 40 μL) were added to the flasks containing the dry DOPC films in order to reach AzoTMA:DOPC weight ratios of either 5:1, 4:1, 3:1, 2:1, or 1:1. After hydrating overnight, the samples were sonicated (Sonics VCX 500 sonicator equipped with a 3 mm stepped microtip, 20% amplitude, 2s burst – 5s rest for 2 min.). Just before DLS measurements, these AzoTMA:DOPC mixed solutions were diluted in water to reach final concentrations as specified in the main text and filtered through Millex Anotop 0.02 μm after dilution.

AzoTMA:DOPC weight ratios between 5:1 and 1:1 correspond to AzoTMA:DOPC mol/mol ratios of 8.5:1 to 1.6:1. Accounting for the equilibrium with surfactant unimers (critical micellar concentration, CMC, of 0.7 to 2.4 g/L depending on compositions and cis:trans isomerization), the effective molar % of AzoTMA in assemblies can however reach values lower than 1 (see section " SAXS studies of mixed assemblies formed in photostationary conditions" in results).

Light scattering

The scattered light intensity was measured at a fixed angle of 90° with a Brookhaven light-scattering instrument (BI-200SM goniometer, BI-9000AT correlator, equipped with a 30 mW laser operating at 637 nm). Decalin was used as a standard to calibrate the intensity.

The light emitting diode (LED) illumination system used for sample irradiation (cooled PE-2, Ropers Scientific) was equipped with diodes, emitting light at 365 and 470 nm, and liquid waveguides. To shine light in the sample cell (*i.e.* from the top of a glass tube of total length 7.5 cm), a pair of silica lenses were installed at the outlet of the waveguide, resulting in a collimated 10 mm diameter light beam. The irradiance of light was 7.2 mW.cm⁻² at 365 nm, or 85 mW.cm⁻² at 470 nm, as measured by an optical power meter (PM100, Thorlabs). Photostationary states under these illumination conditions corresponds to a azoTMA *cis* isomer composition of 64% ± 1% under blue light and 95% ± 2% under UV light [17].

TR-SAXS

All SAXS data was collected at the ID02 beamline at the European Synchrotron Radiation Facility (ESRF) in Grenoble (France)[44], using an integrated in situ LED illumination set-up. In brief, sample were loaded in a capillary of 1.8 mm diameter. X-ray beam size was 0.1 mm x 0.3 mm. The acquisition time per data frame, t_{acq} , was set to < 20 ms to avoid possible radiation damage to the sample. The two-dimensional SAXS patterns were recorded by a Rayonix MX 170 HS CCD detector. The measured SAXS patterns were normalized and azimuthally averaged to obtain the one-dimensional profiles. The background subtracted data are presented as intensity vs modulus of the scattering vector, $Q = (4\pi/\lambda) \sin(\vartheta/2)$, where ϑ is the scattering angle and λ is the X-ray wavelength ($\lambda = 0.995 \text{ \AA}$). The sample-detector distance was 3 m, giving a Q range of 0.003–0.19 \AA^{-1} . Error bars in the regrouped intensity are based on the intensity statistics assuming the Poisson distribution. To further reduce the noise and statistical error bars at high Q , the Intensity data were rebinned in logarithmic steps without losing the Q resolution (*i.e.* retaining all points at lower Q and averaging many points at higher Q).

The LED illumination system (cooled PE-2, Ropers Scientific) equipped with diodes emitting light at 365 and 470 nm was coupled to the SAXS quartz capillary cell (diameter 1.8 mm and wall thickness 10 μm). Silica lenses enabled the light beam to be focused to a spot of ≥ 1 mm diameter at the same position at which the X-ray beam (0.1 mm \times 0.3 mm) crossed the capillary. The total power of the light shining on the capillary (14 mW at 365 nm or 21 mW at 470 nm) was measured with a PM100, Thorlabs optical power meter. The continuous light exposure was synchronized with the SAXS data acquisition using a fast shutter (opening delay < 2.5 ms) placed in the light beam. In this configuration, while the sample was continuously illuminated from the beginning of the acquisition sequence, the X-ray exposure was limited to maximum 20 ms windows. This time was chosen in order to avoid sample radiation damage and/or heating, which was observed at longer continuous exposure times (ex: profile distortion at 100ms exposure). Of note, the light spot was significantly larger than the X-ray spot, thus ensuring photoconversion is constant in all the X-ray probed volume. In addition, diffusion of surfactants and/or micelles could not affect sample's homogeneity in the probed volume. Namely, using typical diffusion coefficients of surfactants unimers and small micelles (of 10^{-6} - $5 \cdot 10^{-6}$ cm^2/s , [45]) the characteristic diffusion time over a distance of the order of the size of the illuminated area (1 mm) is estimated to be of 2000-10000 s. This time is markedly longer than the experimental window used in kinetics measurement.

The reduced and rebinned data [44] were analyzed by fitting analytical scattering models to the experimental SAXS curves. The models used are classical scattering models for vesicles (3-shell model), prolate micelles (prolate core-shell model) and rod-like micelles (cylinder core-shell model) shown in Scheme 1. We have assumed that the hydrophilic part of AzoTMA associates with the hydrophilic part of DOPC to form the shells of the structures, whereas the hydrophobic parts of each component associate to form the core or middle shell of the structures, as illustrated in Scheme 1. Scattering length densities have been calculated using a weighted average of the scattering lengths of the AzoTMA and DOPC tails and headgroup as described in equations (3) and (4) in section S1 of the Supplementary Information (SI). Many of the data sets cannot be described by a single structural model. Optimal fits to some of the experimental curves required a coexistence of two morphologies. In this case we have used models where the scattering from 2 components, ellipsoids + cylinders or cylinders + vesicles, was summed as described in section S1 of the SI. The distribution of lipids and surfactants between the two morphologies was parameterized using two floating molar fractions, χ_{DOPC} being the fraction of the lipid in rod-like micelles and χ_{AzoTMA} the fraction of surfactants in rod-like micelles, respectively. Isolated surfactant molecules (unimers) were also accounted for in the models as described in section S1 of the SI, allowing variations in the CMC of the AzoTMA in the fits. All fit model contributions are described in detail in the SI.

Results and discussion

Light Scattering studies of mixed assemblies in the dark, or exposed to UV or blue light.

We first assessed by light scattering whether the AzoTMA surfactant was capable to solubilize DOPC lipids. Dilute dispersions of DOPC liposomes (0.1 g/L, diameter of about 400 nm) were mixed with increasing concentrations of AzoTMA, below or above the CMC. Addition of *trans* (dark-adapted) AzoTMA did not immediately affect the scattering intensity, but after overnight incubation, most liposomes vanished from samples mixed with AzoTMA in its *trans* isomer form at concentrations above or just below CMC of 0.7 g/L (Table S2.1 in SI). This effect is typically reported for conventional, non-responsive surfactants [46],[47]. The addition of AzoTMA below CMC/2 (< 0.35 g/L) did not modify neither the scattered intensity nor the effective diameter, indicating that most liposomes are not significantly affected by low concentrations of AzoTMA. The CMC of the dark-adapted *trans* isomer is significantly lower than

CMC of the *cis* (UV-irradiated) form (1.8 g/L) [16],[17]. Accordingly, the threshold concentration for liposome solubilization was increased when *cis* isomer was added (Table S2.1). This suggests that in dilute conditions, the *cis* isomer is less prone to associate with DOPC compared to the *trans* one.

	5 g/L		2.5 g/L		1.25 g/L	
	(I-I ₀)/I _{ref}	D (nm)	(I-I ₀)/I _{ref}	D (nm)	(I-I ₀)/I _{ref}	D (nm)
5:1	15.4	5.5*	15.4	6	8.4	6*
4:1	18.3	5.5*	17.8	8.5	4.5	6*
3:1	33.6	10	24.8	25	7.2	14*
2:1	121	29	78.4	33	30.7	30
1:1	704	67	325	57	155	55

Table 1. Characteristic features of mixed AzoTMA:DOPC solutions measured by light scattering. Samples were prepared at the final total concentration (DOPC+AzoTMA) indicated in column headers, and filtered through Millex Anotop 0.02 μm . Samples at 2.5g/L and 1.25 g/L were prepared by dilution in water of the 5 g/L solutions prior to filtration. Intensities were normalized by decalin scattering ($I_{\text{ref}} = 1.7$ kcps). I_0 is the scattering intensity of milliQ water (2.8 kcps). Diameters were estimated either from the second cumulant or (*) by biexponential fits.

Next, AzoTMA:DOPC assemblies were prepared by solubilizing aliquots of dried DOPC lipids with a concentrated *trans*-AzoTMA stock solution (25 g/L). The mixed samples were diluted in water to 5 g/L, 2.5g/L or 1.25 g/L (total weight concentration of DOPC and AzoTMA) and filtered (Anotop 10, pores size of 0.02 μm) to remove dust and/or aggregates hampering the characterization of small micelles by dynamic light scattering (DLS, see method section). Unsurprisingly, an increase in scattering intensity was observed with increasing DOPC content in the mixed samples (Table 1). At a fixed total concentration, increasing the fraction of lipid diminishes the spontaneous curvature of mixed assemblies thus favoring formation of larger, brighter scattering species. This result was consistent with the gradual increase of effective average diameters (Table 1) with increasing fraction of DOPC, also reflected in the gradual shift of the correlation function (Fig. S2.1 in SI). It should be noted that diameters determined by DLS are rough estimates due to i) experimental noise resulting in relative fluctuations of the order of 10%, and ii) the more prominent weight (z-average) of larger species. In solutions enriched in AzoTMA (5:1 and 4:1 wt/wt in Table 1), the effective hydrodynamic diameter was typically lower than 6-7 nm. As a reference, pure AzoTMA surfactant micelles at 5 g/L in the absence of lipids have an overall diameter of around 5 nm (determined by SAXS in [16]). However, at 5g/L the scattering intensity of pure AzoTMA solutions was too low to allow accurate measurements of diameters by DLS. At 20 g/L AzoTMA a diameter of about 3 ± 1 nm was measured by DLS. Of note, diameters larger than the pores of the filter were measured for AzoTMA:DOPC 2:1 and 1:1 mixtures, suggesting that the mixed assemblies were deformable and/or capable to transiently break and reform after filtration. Values of approximately 60 nm hints to the presence of lipidic vesicles or long rod-like micelles that can pass through the filter.

In the experimental conditions, micelles were expected to be present even at the lowest concentration of 1.25g/L, because the CMC of pure *trans*-AzoTMA is 0.7 g/L in water [16],[17]. Somewhat surprisingly, we observed that intensity did not diminish in proportion to concentration in the 5:1, 4:1 and 3:1 mixtures (Table 1), suggesting that upon dilution from 5.0 to 2.5 g/L AzoTMA and DOPC molecules undergo a reorganization toward bigger assemblies. Evolution of the measured diameters also pointed to the formation of larger assemblies at 2.5 g/L compared to 5 g/L solutions. However, the filtration step

(required to remove dust and aggregates) might introduce an experimental bias, retaining or deforming large assemblies such as vesicles. To assess the degree of retention of molecules into filters, AzoTMA was titrated by UV-Vis absorption spectroscopy before and after filtration (Table S2.2). The decrease of absorbance in filtrates of dilute AzoTMA solutions (1.25 g/L with no lipids) showed that the filter membranes can adsorb up to 20 mol% of the surfactant. Cationic surfactants are prone to tight adsorption onto most interfaces. The amount of loss in the filter was essentially negligible in samples at 5 g/L and 2.5 g/L, including in samples containing a predominant fraction of AzoTMA (Table S2.2). This suggests that mixed-assemblies with low DOPC content can fully pass through filters. In contrast, AzoTMA:DOPC 1:1 solutions were always partially retained into the filters, not only at 1.25 g/L but also at higher concentrations (2.5 and 5 g/L). A loss of 10-15% mol of AzoTMA was observed for 1:1 solutions at 2.5 or 5 g/L, suggesting that these samples contained assemblies larger than the pore size of the filter.

Finally, the samples were irradiated for 10 min with UV light (365 nm) directly in the DLS measurement cell. Solutions at 1.25 g/L reached the photostationary state enriched in *cis*-AzoTMA isomer after a few minutes of UV light irradiation (see Fig S2.2). A decrease of light scattering intensity was observed when UV light was shone on all the samples at 1.25 g/L. Exposure to blue light (470nm) after this UV light treatment increased the light scattering almost back to its initial value (Fig. 1). Alternating UV and blue light exposures, and accordingly *trans-cis* / *cis-trans* isomerization cycles, produced reversible changes in AzoTMA:DOPC assemblies (Fig. 1). Assuming that the scattered intensity varies with both the weight concentration and average molar mass of species, the ratio of photoinduced variations of scattered intensity $\Delta = (I_{UV} - I_w) / (I_{blue} - I_w)$ gives an index of growth and/or appearance of scattering species. Values of Δ lower than 1 suggests that exposure to UV triggered disassembling and/or release of AzoTMA unimers in solution. The decrease of Δ from 0.8 to 0.6 with increasing fraction of DOPC (Table S2.3) in addition suggests that in larger assemblies the photo-destabilization/disassembling was more pronounced. It was unfortunately not possible to determine average diameters under UV light because the laser of the light scattering instrument (637 nm, 30 mW) triggered a slow *cis-to-trans* back-isomerization of AzoTMA. Attempts to record data at lower laser intensities (3 mW) led to noisy correlation functions in samples containing small micelles. When diameters could be estimated, they were of similar order of magnitude under UV light as in dark-adapted samples.

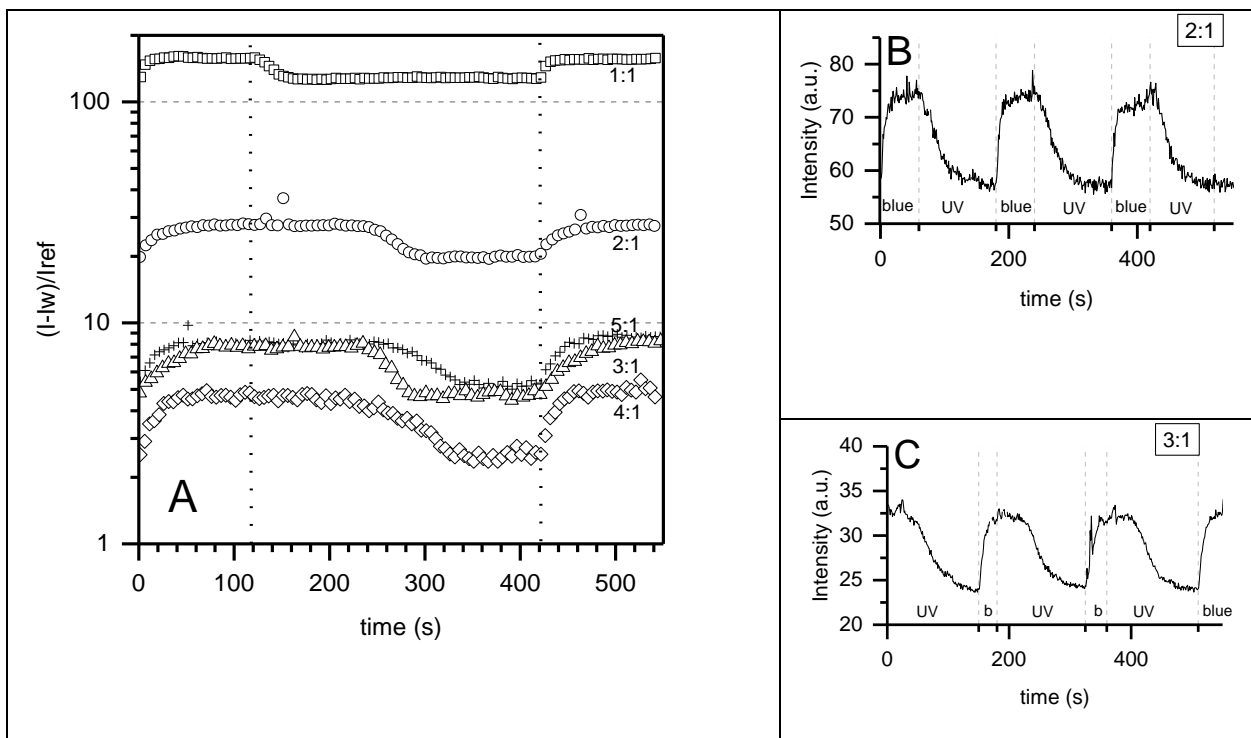


Figure 1. Intensity scattered by 1.25 g/L AzoTMA:DOPC mixed solutions irradiated under blue (470 nm) or UV light (365 nm). Samples quoted in figures were pre-irradiated under UV light for 10 min. (A) blue light was shone from time zero to 120 s, and from 420 s to 550 s; UV light between $t=120$ s and 420 s (dotted vertical line); (B) cycles of irradiation with alternating blue/UV light as quoted by dashed lines. lw = intensity scattered by water, I_{ref} = intensity scattered by decalin.

SAXS studies of mixed assemblies formed in photostationary conditions

Compared to light scattering, SAXS is better suited to characterize the lipid-surfactant assemblies in detail as it grants information on the morphology (e.g. spheroidal, rod-like micelles or vesicles) as well as the detailed structural dimensions. In addition, no filtration step is needed, avoiding possible composition bias (due to adsorption in the filter membranes). We recorded SAXS profiles of the same preparations as in Table 1 and Fig. 1, but with no filtration, either in the dark ("dark-adapted") or after exposure to UV or blue light. Three models of assemblies have been used to fit the experimental data: spheroid micelles, rod-like micelles and vesicles (Scheme 1), as described in the experimental section and detailed in SI. Results of the fits enabled identification of the predominant species present as a function of compositions and irradiation conditions as summarized in Figure 2. In the cases where a single geometrical model was found to fit the data, the main fitted parameters were the core radius and shell thickness, whereas degree of interphase smearing ($< 0.5\text{nm}$), as well as the density of the lipid and surfactant tailgroups were used to refine the match to data. The densities of the full molecules (both DOPC and AzoTMA) were kept constant according to literature data (see legend in Table SI1.3 in SI). In other cases, we choose to enable a coexistence of two structures, and the fractions of lipid and surfactant distributed in each structure were introduced as two new fit parameters. The aforementioned structural parameters were floated for each structure, while the same molecular densities were used for both assemblies. Coexistence of vesicles and rod-like micelles is typical of intermediate compositions in lipid:surfactants mixtures.[47]-[48] Coexistence of small spheroidal micelles and rod-like mixed micelles made of surfactants and lipids have also been reported: first as intermediate transient stages during the transition from spheroids to cylinders (e.g. in the case of SDS micelles,[37],[38] and second in the case of cationic surfactants and low ionic strength, [47], [48] that resemble the present AzoTMA:DOPC system. The choice of fitting some data by bimodal population of

spheroids and rods was accordingly motivated by these previous reports, though we did not rule out that alternative models, such as highly polydisperse thread-like micelles could match our data as well. Our goal was not to establish this coexistence, but to compare characteristic structural features observed in static/stationary conditions with the transient stages of the photo-triggered kinetics. Detailed structural parameters as well as the model fits to the experimental SAXS curves are shown in Figure 3 and SI Tables S3.1 and S3.2.

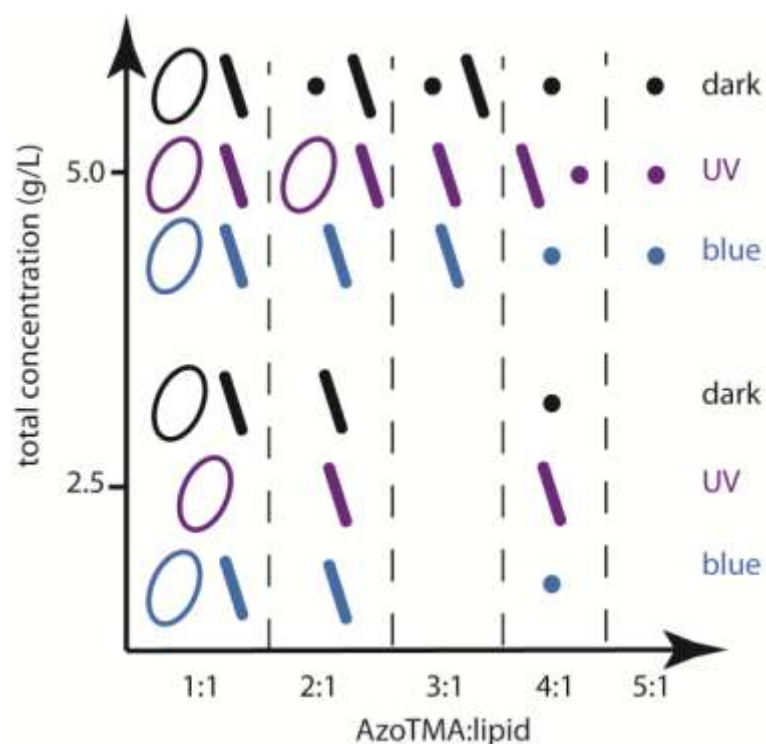


Figure 2. Diagram of the predominant morphologies found in photostationary conditions as determined by SAXS of wt/wt mixtures at 5 g/L or 2.5 g/L total AzoTMA:DOPC concentration. Black, blue, and purple colors respectively point to dark-adapted (100% trans-AzoTMA), blue light, or UV-light irradiated samples. Spheroid micelles: full circles, rod-like micelles: thick lines, vesicles: empty ellipses.

For dark-adapted (100% trans azobenzene) AzoTMA:DOPC at 5:1 and 4:1 g/g, the scattering at low Q-values clearly point to the presence small structures in solution, similar to that of pure AzoTMA micelles albeit with a different scattering length density due to the incorporation of lipids. In this case, we modified the prolate micelle model previously used for the AzoTMA micelles [13] to include the lipid scattering, which fitted better to the experimental data (Fig. 2, radius of about 2.8 - 3.0 nm and core aspect ratio of 2.4 - 2.6 see Table S3.1). These mixed micelles are very similar to micelles of pure AzoTMA (that have the same radius but an aspect ratio around 1.2) [16]. At higher DOPC fractions, the slope in the low Q region gradually changes, indicating larger structures that still maintain the similar core-shell morphology of micelles. SAXS analysis revealed that the introduction of rod-like elongated micelles best described this change, giving a co-existence between small spheroidal and rod-like micelles in AzoTMA:DOPC 3:1, whereas rod-like micelles were predominant in the 2:1 mixture. Finally, in the 1:1 mixtures the scattering pattern in the intermediate and low Q-range is clearly wider than that of the lower ratios, resembling the typical bilayer scattering. A model including vesicles in coexistence with rod-like micelles fitted best in the 1:1 mixtures. The Q-range as well as the polydispersity smearing of the spherical form factor do not allow us to decisively determine whether the structure is actually vesicles or large free-floating bilayers. We opted for the vesicles, as it has already been reported for ionic surfactants at low ionic strength [49], but apparent diameter of vesicles must here be considered as a dummy parameter. Interestingly, the relevant

structural parameters of either three types of assemblies were little affected by the AzoTMA:DOPC mixing ratio. In 5:1, 4:1 and 3:1 mixtures, spheroidal micelles have a radii between 1.9 and 2.2 nm and shell thicknesses between 0.9 and 1.2 nm. Similarly, variations of the parameters by < 10% matched with fits of rod-like micelles that are present in 3:1, 2:1 and 1:1 samples (core radii between 1.8 and 2.0 nm, shell thicknesses between 0.9 and 1 nm, lengths between 24 and 31 nm). This remark also holds true for radii of micelles and rods observed at 2.5 g/L, though rods appeared to be longer in dilute solutions and the region of coexistence between spheroidal and rod-like micelles was not observed in the more dilute samples. Additional information extracted from the fit concerns the concentration of unimers of AzoTMA (i.e. isolated surfactant molecules) indicated as the effective CMC in Table S3.1 in SI. The change in CMC was determined from by the change in the total scattering that cannot be ascribed to micellar or vesicle structures in the SAXS data. The effective CMC in the dark (100% trans) did not vary significantly as long as the surfactant was predominant. This result suggests that the equilibrium of unimers with mixed assemblies is not markedly different than with self-assemblies of pure AzoTMA in 5:1, 4:1 and 3:1 samples. In contrast, the effective CMC decreased significantly in 2:1 and 1:1 mixtures, reflecting that at the onset of vesicle formation the chemical environment of AzoTMA incorporated into the assemblies with DOPC is significantly different from pure AzoTMA micelles.

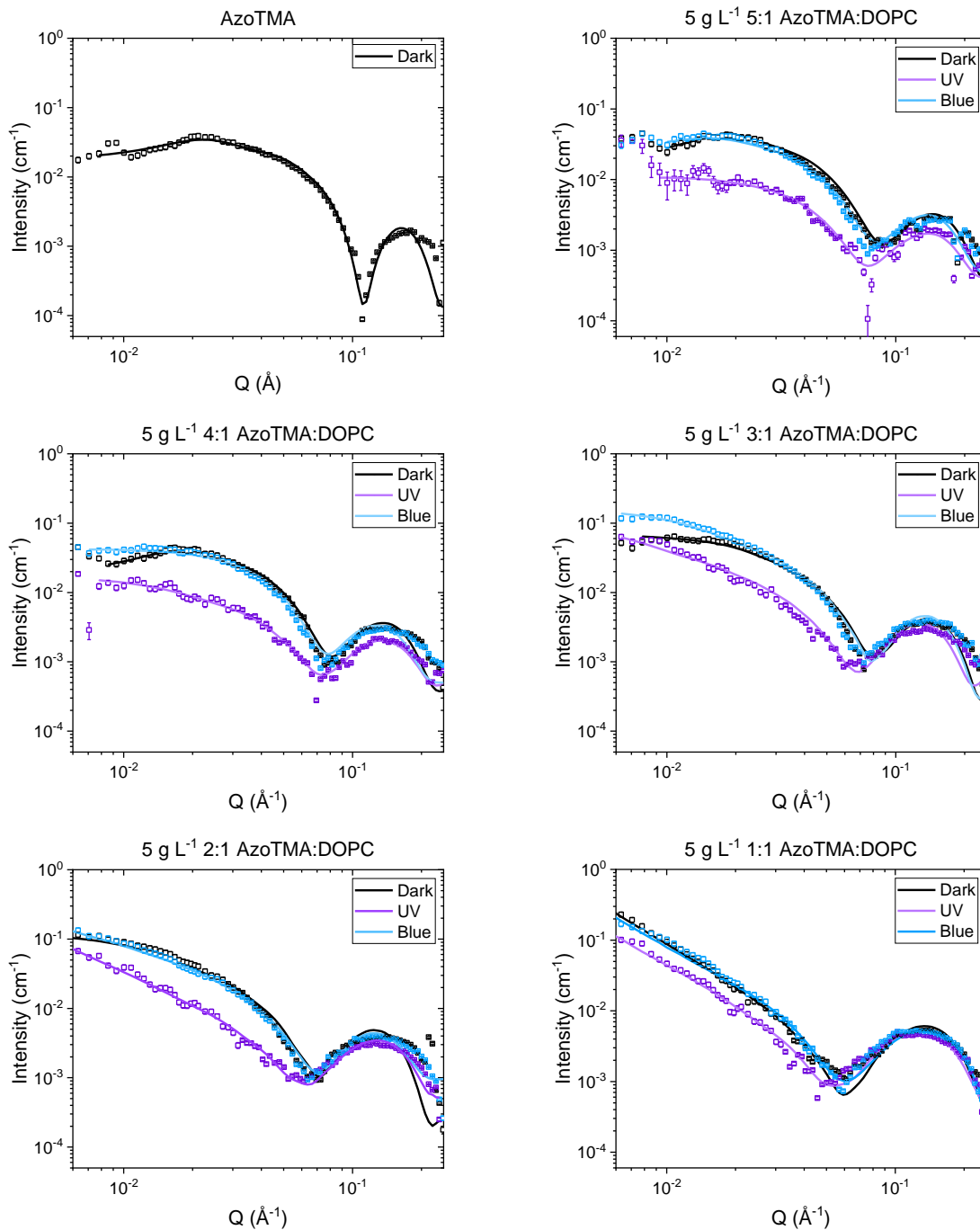


Figure 3. SAXS profiles and model fits for the samples at 5 g/L at different AzoTMA/DOPC compositions and irradiation conditions. Full dots represent experimental data and the lines are the best fits. Dark state is represented in black, photostationary state reached after UV or Blue irradiation are represented in purple or blue, respectively. When not specified, error bars are smaller than symbols

After equilibration under UV light irradiation, the fitted parameters were modified as compared to the dark-adapted state. The general trend was a clear increase of effective CMC by a factor of ~ 3 (from 0.7 g/L to about 2.3-2.6 g/L, except in 1:1 mixture where it varied from 0.4-0.6 g/L up to 1.1-1.2 g/L). This suggests a photo-release of AzoTMA unimers to the bulk solution, likely in their *cis* isomer form. Exposure to UV light also increased the relative fraction of rod-like micelles in 4:1 and 3:1 mixtures, and promoted formation of vesicles in 2:1 and 1:1 mixtures. Finally, at the highest dilution and highest fraction of DOPC analyzed by SAXS (AzoTMA:DOPC 1:1, 2.5 g/L), mixed rod-like micelles and vesicles became a dispersion of pure vesicles after UV exposure. This is consistent with typical phase transitions of amphiphiles with longer

rod-like micelles appearing on the verge of the transition to coexistence with vesicles [47]. The photostationary state reached after exposure to blue light was intermediate between the UV and dark-adapted ones, suggesting a partial recovery of smaller assemblies (spheroid or short rod-like micelles) when *cis* isomers are photoconverted to *trans* ones. Interestingly, the characteristic radii of the mixed micelles did not significantly vary in these various conditions, either after exposure to UV or blue light. This result suggests that photoconversions essentially modifies the mass fractions of the assemblies without significantly affecting their morphologies. Namely, the core radius of spheroid micelles was in the window of 1.9 nm -2.2 nm. The core radius of rod-like micelles was between 1.8-2.0 nm (Table S3.1).

Altogether, results from SAXS analysis of mixtures that were equilibrated in the dark, or in photostationary conditions, primarily indicate that DOPC:AzoTMA assemblies resemble conventional mixed systems of lipids and surfactants. Typically, depending on the chemical nature of the amphiphiles, when increasing the fraction of lipid molecules, conventional mixed systems undergo transitions from spheroid-like micelles to vesicles [50] or spheroid/rod-like micelles to vesicles [49, 51]. Entering into a detailed picture of typical morphologies formed at intermediate compositions may actually be quite complicated, and feature the coexistence of several mixed assemblies [52]. We can, however, compare our observations of intermediate objects with typical predominant morphologies. The representative transitions observed while increasing the fraction of surfactant such as Triton X100, or alkyl-PEO mixed with phospholipids are: 1) intermediate vesicles of various diameters, with gradual increase of membrane defects such as pores that grow in size and/or number resulting in dispersions of cup-like vesicles or quasi-planar bilayers up to a saturation threshold of the lipid membranes by the surfactant; 2) beyond saturation long rod-like micelles coexisting with membrane sheets; 3) finally, disappearance of all membranes, and shortening of the rod-like micelles to ultimately end with almost spherical micelles. With ionic surfactants (sodium dodecyl sulfate, cetyltrimethyl ammonium chloride) these intermediate morphologies are slightly different [47],[48],[49], [52]. In this case, no cup-like lamellae are observed, but instead highly porous membranes (called perforated vesicles or stomatosomes) evolve via an increase of pore diameters and thinning of inter-pore walls. When the rims of the pores become the predominant structures, these assemblies are like networks of branched, interconnected rod-like micelles. Of note, highly porous, perforated vesicles were typically observed in brine (NaCl > 100mM). In the absence of salt, the vesicle to rod-like micelle transition occurs with no obvious intermediate perforations. In addition, vesicle, rod-like and small quasi-spherical micelles may coexist at low ionic strength [49]. In particular, coexistence of small and elongated micelles is generally not reported with neutral surfactants, or ionic ones in the presence of salt, but can occur in ionic systems at low salt. Finally, coexistence of vesicles, rod-like and spheroid micelles follows the typical sequence reported in the literature cited above. Coexistence of small spheroid micelles and rods is in addition consistent with the cationic nature of AzoTMA head group, similar to the head of alkyl-trimethyl ammonium, and with assemblies in water (in the absence of salt).

As an intermediate conclusion, results in static conditions indicate accordingly that *trans-to-cis* photoisomerization plays a similar role as AzoTMA dilution: it diminishes the fraction of surfactant bound into lipid assemblies thus favoring low-curvature assemblies. Due to the increase of CMC with *trans-to-cis* isomerization, the effective fraction of surfactant bound into DOPC-containing assemblies is lowered under UV exposure as compared to the dark or blue-exposed samples of the same composition. The fitted values of CMC and fractions of AzoTMA in the various assemblies enabled to quantify the effective molar fractions of AzoTMA and DOPC in the diverse assemblies. In spheroid micelles the highest DOPC/AzoTMA ratio was reached under UV in the presence of *cis*-AzoTMA (0.27 mol/mol, as compared to 0.14-0.17 mol/mol in the

dark-adapted state). In rod-like micelles, the DOPC/AzoTMA ratio was of 0.7 mol/mol under UV, and about 0.5 mol/mol in samples predominantly containing *trans*-isomer (in the dark or under blue light). Within variation of fitted parameters values of ca. 10%, these compositions of assemblies were the same in all samples.

Time-resolved evolution of AzoTMA:DOPC mixtures exposed to light.

We used TR-SAXS to analyze the kinetics of intermediate reorganization during *trans-cis* isomerization in samples at 5 g/L, and recorded multiple SAXS patterns during continuous UV or blue light irradiation. Our working hypothesis was that if the azobenzene isomerization is a limiting step of the kinetics, the morphologies observed in static conditions will be also the main assemblies present at all time. We accordingly assessed that the full set of intermediate SAXS profiles could be fitted to a model with a minimum of adjustable parameters, *i.e.* simply by adjusting CMC, and the fractions χ_{AzoTMA} and χ_{DOPC} . χ_{AzoTMA} (resp. χ_{DOPC}) is the molar ratio of AzoTMA (resp. lipid) present in rod-like micelles to the total amount of AzoTMA (resp. lipid). The remaining fraction ($1 - \chi_{\text{AzoTMA}}$) correspond to AzoTMA either present as unimers, and/or in spheroidal micelles and/or in vesicles depending on the samples. The other structural parameters (mean size, core radius and shell thickness, surfactant and lipid densities, *etc.*) were kept constant in the first round of the fitting procedure. Then, the fits were refined by allowing variation of the core radii and shell thicknesses, vesicle radii and lipid and AzoTMA packing densities (Figure S3.2). This second step produced only small variations (< 10%) of the fit quality, and minor (<10%) changes in the values of structural parameters. The initial and final states of the kinetics match, within experimental uncertainties the values of the parameters determined in photostationary samples (Table S3.2).

When UV light was shone on the samples, CMC increased with time until a photo stationary state is reached (Figure 4A). A characteristic relaxation time, τ , was estimated by fitting data to a monoexponential function ($\tau = 68 \pm 11$ s for 1:1, $\tau = 48 \pm 8$ s for 2:1 and 40 ± 10 s for 4:1 sample). The response time was of the order of the *trans* to *cis* isomerization time measured in 5 g/L AzoTMA solutions in similar conditions [16]. The decrease of the rate of CMC variation with increasing DOPC fraction was close to experimental uncertainty, but statistically relevant. This variation of the response time of the CMC may be reflecting a change in the rate of *trans*-to-*cis* photoisomerization, which has been reported to be slowed down in a lipid environment [21]. Exposure to UV light in addition induced the redistribution of AzoTMA and DOPC between the small and rod-like micelles or between micelles and vesicles. Typically, the AzoTMA:DOPC 2:1 mixture contained at $t=0$ small spheroid micelles mixed with rod-like ones, that evolved first to rod-like micelles before ending up as a mixture of vesicles and rod-like micelles (Fig. S3.3). Interestingly, the time of appearance or disappearance of the mixed assemblies did not simply follow the characteristic time of CMC variation. In 4:1 mixture, the formation of rod-like micelles did not start until the CMC variation was almost completed, *i.e.* once the release of the AzoTMA unimers has reached its maximum. The corresponding lag time of approximately 100 s, evidenced in the plot of χ_{DOPC} and χ_{AzoTMA} vs time (Fig. 4B), reflects that spheroid micelles gradually lose AzoTMA molecules and are enriched in DOPC without marked variation of their (small) radii. Thus, the delay in micellar elongation, and the abrupt appearance of rod-like micelles presumably indicate that below a threshold DOPC/AzoTMA ratio small micelles are the most stable form. The evolution of 2:1 mixture similarly suggests that vesicle formation is observed after a lag time. In this case, while CMC was changing gradually, the spheroid micelles quickly disappeared in the initial states of the irradiation to yield almost 100% rod-like micelles, which persisted for a few tens of seconds. Vesicles abruptly emerged, presumably when a threshold composition of the rod-like micelles was crossed (Figure

S3.3). In contrast, when both vesicles and rod-like micelles coexisted at time zero (1:1 mixture), no delay was observed and an increase of the fraction of vesicles (shown by a decrease of χ_{DOPC} and χ_{azoTMA}) started immediately when light was switched on (Fig. S3.4).

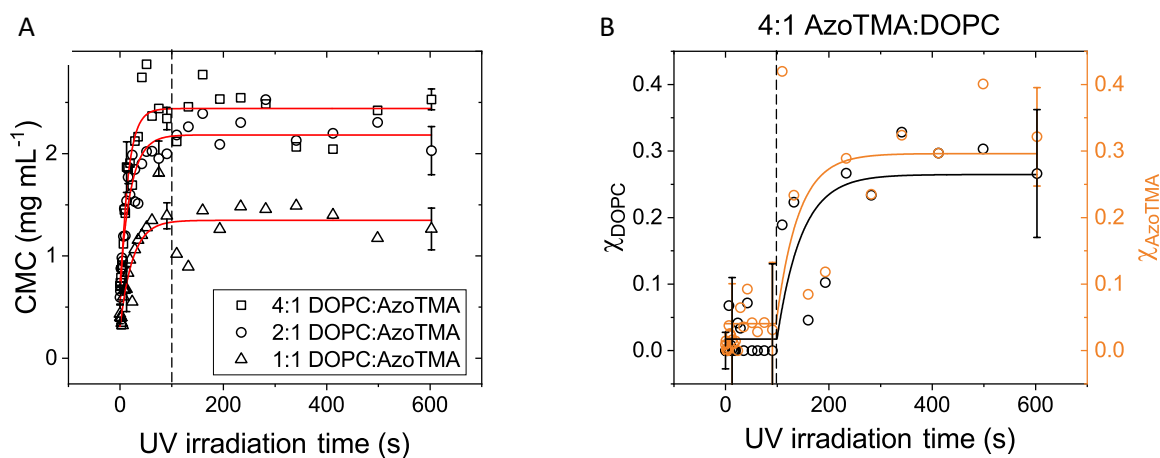


Figure 4. Dark-adapted AzoTMA:DOPC (5 g/L) reorganization kinetics under UV exposure as observed by TR-SAXS a) CMC variation and b) χ_{AzoTMA} and χ_{DOPC} (i.e. fractions of respectively surfactant and lipid present into rod-like micelles as compared to their total amount in all other forms in AzoTMA:DOPC 4:1 mixture. In this case, the remaining fraction, $1-\chi$, is mainly present as spheroidal micelles. The error bars have been estimated as the upper and lower values obtained at the end of fitting procedures launched using extremes in initial parameters.

To assess the backward pathways triggered by *cis* to *trans* isomerization, UV-adapted samples (UV-light exposed for > 10 minutes) were irradiated by blue light. At the intensity of blue light shone in the cell *cis* to *trans* isomerization was expected to be completed at second time scale (see [16]), significantly faster than the *trans*-to-*cis* UV-triggered photoconversion. Accordingly, the decrease of the CMC took place within less than one second (Fig. 5A). This response time was much faster than minimum sampling time needed to collect SAXS profiles with reasonable statistics. Interestingly, the redistribution of AzoTMA and DOPC between the micelles and vesicles or between rod-like and spheroid micelles started immediately in samples initially containing a mixture of assemblies, and required 5 to 10 s to be completed. This remark holds true, for example, in UV-adapted 2:1 AzoTMA:DOPC mixtures containing rod-like micelles and vesicles (Fig. 5A), 1:1 mixtures containing vesicles and rod-like micelles (Fig. S3.4), or in 4:1 containing spheroid and rod-like micelles (Fig. S3.5 in SI). In all these cases, the rate of CMC variation was faster than any morphological reorganisation. Because the effective CMC reflects the degree of association of unimers with the assemblies, this suggests that the equilibrium with the unimers in solution was not the rate limiting process. Variation at time scales of a few seconds presumably reveals a slow equilibration process of the respective lipid/surfactant ratios between vesicles and micelles.

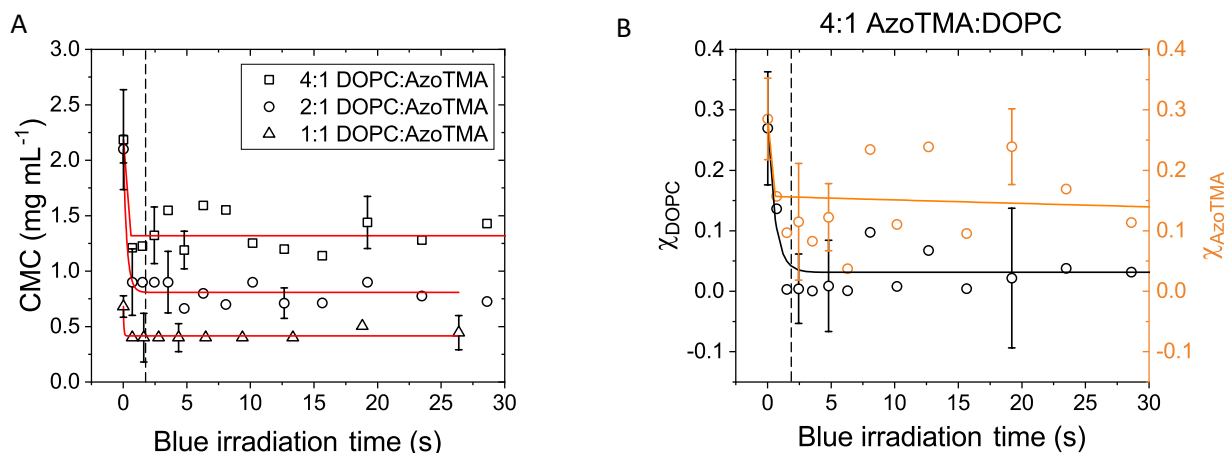
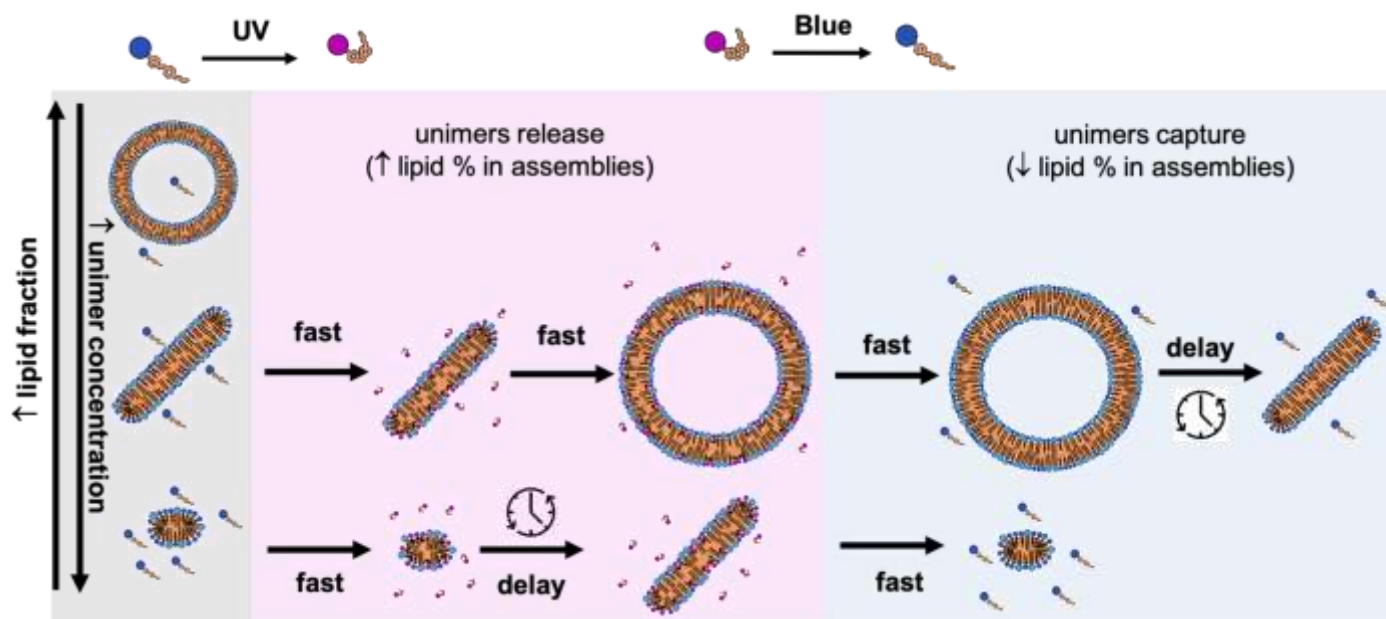


Figure 5. UV-adapted AzoTMA:DOPC (5.0 g/L) reorganization kinetics under blue exposure as observed by TR-SAXS a) CMC variation and b) χ_{AzoTMA} and χ_{DOPC} fractions in rod-like micelles in AzoTMA:DOPC 2:1 mixture (see legend of Fig. 4. The error bars have been estimated from the upper and lower values obtained at the end of fitting procedures launched using extremes in initial parameters.

In summary, photoperturbation of lipid-surfactant mixtures triggers kinetics that were captured by a simple redistribution between three main components: small spheroid micelles, rod-like micelles, and vesicles that resemble the equilibrium assemblies. Accordingly, the model suggests that intermediate states pass across a sequence of solution composition that is also followed by a gradual variation of the DOPC/surfactant ratio. Typically, *trans* to *cis* isomerization is shown to deplete micelles from AzoTMA, changing the effective packing parameter and triggering either formation of rod-like micelles from a solution containing small micelles, or appearance of vesicles from solution initially containing rod-like micelles (scheme 2). From a physical chemistry point of view, these transitions correspond to a shift towards higher average packing parameter of the amphiphilic molecules, driven by the isomerization of the azobenzene. Photoisomerization of *trans* to *cis* AzoTMA causes a variation of the specific area that the surfactant tail occupies, as measured by Lee and Hatton [53]. Thus, *cis* isomerization of AzoTMA decreases the molecular density at interfaces. Because the hydrophilic head of AzoTMA remains constant upon photoisomerization, this result suggests a decrease of the thickness of the hydrophobic layer, *i.e.* an increase of the packing parameter. Similar simulations on azobenzene surfactants indicate that the *cis* isomer creates a “kink” in their hydrophobic tail, making the hydrophobic layer markedly thinner [54] as compared to the highly packed and thick layer created by stacks of pure *trans* molecules. Similar photovariation of the molecular packing parameter were also consistently reported in other azo-containing surfactants (in the absence of lipids) and associated in literature to similar variations of interfacial properties and/or transitions from small micelles to cylinders [55] [56]. Our analysis of photostationary states validates the optical control of the intrinsic/spontaneous curvature for mixed assemblies of lipids and azo surfactants. Kinetic measurements provide new information on the typical reorganization time of the mixed assemblies. Because the lipid reorganization between water and assemblies is much longer than our experimental time, reorganization mainly depends on i) partition of azoTMA between unimers and assemblies, ii) evolution time(s) of lipid-containing assemblies. In addition, lag times observed in samples with an initial predominant component (either spheroid micelles or cylinders) are presumably indicative of the irradiation time required to reach a *cis:trans* threshold composition, *i.e.* a critical spontaneous curvature in mixed structures, to trigger the coexistence of micelles with cylinders or cylinders with vesicles. The existence of such a threshold is typically reported in lipid:surfactant co-micellization, and characterizes the coexistence windows between two microphases containing respectively, a high lipid or

low lipid fraction. [50],[46] Finally, the blue light-triggered switch was fast enough to observe non-equilibrium structures. In this case, the fast *cis*-to-*trans* isomerization revealed that AzoTMA unimers in solution quickly reach an equilibrium state, at time scales shorter than our sampling time, before any morphological equilibration occurs (here between micelles and/or vesicles). This result suggests that the morphological transition between rod-like micelles and vesicles can be estimated as a slow process, with a characteristic time of a few seconds. Due to the shear sensitivity of long rod-like micelles and vesicles, those kinetics observations could not be obtained by alternative fast mixing processes, such as stop-flow. In addition, light-responsive surfactant provides a unique possibility to specifically target properties changes on the surfactant, without affecting the lipids.



Scheme 2. structural dynamics of photo-controlled reorganizations of azoTMA:lipid mixed assemblies

Conclusion.

We prepared mixed lipid:cationic azobenzene-containing surfactant (azoTMA) solutions in a number of equilibrium states and non-equilibrium transient stages by controlling in situ the association/dissociation features of *trans*/*cis* photoisomers of AzoTMA. Light enabled us to reversibly switch between different morphologies of their mixed assemblies. Using TR-SAXS combined with the specific optical perturbation targeting the surfactant, we found that the partitioning of surfactant unimers in water precedes the mass reorganisation at mesoscale. As we achieved variations of *cis*:*trans* isomers, which were faster or on time scale similar to the reorganization time of the assemblies, this finding complements the present literature that up to now addressed kinetics that were rate-limited by the amount of photoisomers produced in solution.[12],[13, 14]

Using SAXS we determined the structural parameters of 3 characteristic assemblies: small ellipsoidal micelles, rod-like micelles, and mixed unilamellar vesicles. Their structural parameters (radii and aspect ratio of small micelles, cross-section of rod-like micelles, or membrane thickness of vesicles) did not markedly depend on composition of samples, suggesting that equilibrium was primarily reached by a redistribution of molecules among these three, essentially fixed, characteristic structures. Interestingly, the coexistence of well-defined small micelles with rod-like micelles was observed and recognized as typical of

mixed systems of cationic surfactants at low ionic strengths. The perturbation introduced by shining light on pre-equilibrated samples enabled to record kinetics-of the evolution of the assemblies between the equilibrium states and/or photostationary states. Existence of out-of-equilibrium intermediate states with other morphologies than the ones found in equilibrium were not required to fit the experimental data. In particular, the kinetic pathways could be described as a gradual redistribution between these 3 main components (with slightly adjustable length of the rods and/or diameter of vesicles) whose outer and core radii were remarkably stable. These results suggest that a simplified but robust 3-state model is effective to account for the time-resolved perturbations introduced by photo-triggered changes on mixed lipid:surfactant assemblies. The model enabled us to follow variations of the effective CMC (i.e. surfactant unimer concentration) and of the relative fraction of lipids and surfactants in the different assemblies. We found a few cases showing slower rate of morphological reorganisation as compared to equilibration rate with AzoTMA unimers, i.e. out-of-equilibrium transient situations achieved by shining light (at the intensities produced by non-laser, LED-based set-ups). This slow reshaping, taking up to a few seconds in the presence of lipids in mixed assemblies contrasts with the faster equilibration (< ms) between unimers and micelles of pure surfactants. As compared to fast mixing stopped-flow and temperature-jump techniques, the present approach specifically target photo-sensitive molecules in samples at rest, thus being relevant to investigate soft (ex. shear-sensitive) colloids in non-equilibrium conditions. Namely, stimuli-responsive capsules used in drug delivery are typically made of non-responsive lipids and one stimuli-responsive amphiphile.[10],[19-24] It is of general interest for the design of such systems to study how the presence of lipids slows down kinetics of molecular exchange and/or determines the rate of morphological reorganization. Here, the kinetics of the process, whereby AzoTMA unimer exchange precedes the morphological transitions is an important consideration to guide the design of fast-responsive assemblies such as lipid capsules for drug delivery. Further investigations of pore formation in lipid:azosurfactants membranes have to be conducted at similarly short time scales to determine implications of the non-equilibrium, transient dynamics in the lipid membranes of these capsules.

Acknowledgments.

We acknowledge funding from the 'Initiative d'Excellence' program from the French State (Grant 'DYNAMO', ANR-11-LABEX-0011-01) and from the ANR GenCap (ANR-17-CE09-0007). The ESRF is thanked for the provision of beam time SC-4184.

Author's contribution: All authors contributed to writing, editing and revising ; J. Royes: Investigation, Formal analysis, Visualization ; V. Bjørnstad: Software, Formal analysis ; G. Brun: Investigation ; T. Narayanan : Methodology ; R. Lund: Supervision, Investigation, Methodology, Funding ; C. Tribet: Conceptualization, Supervision, Investigation, Funding

References.

- [1] X.Y. Liu, N.L. Abbott, Spatial and temporal control of surfactant systems, *Journal of Colloid and Interface Science* 339(1) (2009) 1-18.
- [2] P. Brown, C.P. Butts, J. Eastoe, Stimuli-responsive surfactants, *Soft Matter* 9(8) (2013) 2365-2374.
- [3] S. Santer, Remote control of soft nano-objects by light using azobenzene containing surfactants, *Journal of Physics D-Applied Physics* 51(1) (2018).
- [4] S. Chen, R. Costil, F.K.-C. Leung, B.L. Feringa, Self-Assembly of Photoresponsive Molecular Amphiphiles in Aqueous Media, *Angewandte Chemie International Edition* [10.1002/anie.202007693](https://doi.org/10.1002/anie.202007693)(n/a) (2021).
- [5] H. Oh, A.M. Ketner, R. Heymann, E. Kesselman, D. Danino, D.E. Falvey, S.R. Raghavan, A simple route to fluids with photo-switchable viscosities based on a reversible transition between vesicles and wormlike micelles, *Soft Matter* 9(20) (2013) 5025-5033.
- [6] A.M. Ketner, R. Kumar, T.S. Davies, P.W. Elder, S.R. Raghavan, A simple class of photorheological fluids: Surfactant solutions with viscosity tunable by light, *Journal of the American Chemical Society* 129(6) (2007) 1553-1559.
- [7] D. Yang, M. Piech, N.S. Bell, D. Gust, S. Vail, A.A. Garcia, J. Schneider, C.-D. Park, M.A. Hayes, S.T. Picraux, Photon control of liquid motion on reversibly photoresponsive surfaces, *Langmuir* 23(21) (2007) 10864-10872.
- [8] E. Chevallier, C. Monteux, F. Lequeux, C. Tribet, Photofoams: Remote Control of Foam Destabilization by Exposure to Light Using an Azobenzene Surfactant, *Langmuir* 28(5) (2012) 2308-2312.
- [9] S. Khoukh, P. Perrin, F. Bes de Berc, C. Tribet, Reversible Light-Triggered Control of Emulsion Type and Stability, *ChemPhysChem* 6(10) (2005) 2009-2012.
- [10] N. Basílio, L. García-Río, Photoswitchable vesicles, *Current Opinion in Colloid & Interface Science* 32 (2017) 29-38.
- [11] D. Baigl, Photo-actuation of liquids for light-driven microfluidics: state of the art and perspectives, *Lab on a Chip* 12(19) (2012) 3637-3653.
- [12] M. Akamatsu, P.A. FitzGerald, M. Shiina, T. Misono, K. Tsuchiya, K. Sakai, M. Abe, G.G. Warr, H. Sakai, Micelle Structure in a Photoresponsive Surfactant with and without Solubilized Ethylbenzene from Small-Angle Neutron Scattering, *Journal of Physical Chemistry B* 119(18) (2015) 5904-5910.
- [13] R.F. Tabor, M.J. Pottage, C.J. Garvey, B.L. Wilkinson, Light-induced structural evolution of photoswitchable carbohydrate-based surfactant micelles, *Chemical Communications* 51(25) (2015) 5509-5512.
- [14] E.A. Kelly, J.E. Houston, R.C. Evans, Probing the dynamic self-assembly behaviour of photoswitchable wormlike micelles in real-time, *Soft Matter* 15(6) (2019) 1253-1259.
- [15] B.A. Ciccirelli, J.A. Elia, T.A. Hatton, K.A. Smith, Temperature dependence of aggregation and dynamic surface tension in a photoresponsive surfactant system, *Langmuir* 23(16) (2007) 8323-8330.
- [16] R. Lund, G. Brun, E. Chevallier, T. Narayanan, C. Tribet, Kinetics of Photocontrollable Micelles: Light-Induced Self-Assembly and Disassembly of Azobenzene-Based Surfactants Revealed by TR-SAXS, *Langmuir* 32(11) (2016) 2539-2548.
- [17] E. Chevallier, A. Mamane, H.A. Stone, C. Tribet, F. Lequeux, C. Monteux, Pumping-out photo-surfactants from an air-water interface using light, *Soft Matter* 7(17) (2011) 7866-7874.
- [18] D. Feldmann, S.R. Maduar, M. Santer, N. Lomadze, O.I. Vinogradova, S. Santer, Manipulation of small particles at solid liquid interface: light driven diffusioosmosis, *Scientific Reports* 6(1) (2016) 36443.
- [19] J.M. Kuiper, J. Engberts, H-aggregation of azobenzene-substituted amphiphiles in vesicular membranes, *Langmuir* 20(4) (2004) 1152-1160.
- [20] R.H. Bisby, C. Mead, C.G. Morgan, Wavelength-Programmed Solute Release from Photosensitive Liposomes, *Biochemical and Biophysical Research Communications* 276 (2000) 169-173.
- [21] X.-M. Liu, B. Yang, Y.-L. Wang, J.-Y. Wang, Photoisomerisable cholesterol derivatives as photo-trigger of liposomes: Effect of lipid polarity, temperature, incorporation ratio, and cholesterol, *Biochimica et Biophysica Acta* 1720 (2004) 28-34.
- [22] Y. Ohya, Y. Okuyama, A. Fukunaga, T. Ouchi, Photo-sensitive lipid membrane perturbation by a single chain lipid having terminal spiropyran group, *supramolecular science* 5 (1998) 21-29.
- [23] A. Yavlovich, A. Singh, R. Blumenthal, A. Puri, A novel class of photo-triggerable liposomes containing DPPC:DC8,9PC as vehicles for delivery of doxorubicin to cells, *Biochimica Biophysica Acta-Biomembranes* 1808(1) (2011) 117-126.
- [24] N.L. Mutter, J. Volaric, W. Szymanski, B.L. Feringa, G. Maglia, Reversible Photocontrolled Nanopore Assembly, *Journal of the American Chemical Society* 141(36) (2019) 14356-14363.
- [25] T. Hamada, Y.T. Sato, K. Yoshikawa, T. Nagasaki, Reversible Photoswitching in a Cell-Sized Vesicle, *Langmuir* 21(17) (2005) 7626-7628.

- [26] C. Pernpeintner, J.A. Frank, P. Urban, C.R. Roeske, S.D. Pritzl, D. Trauner, T. Lohmuller, Light-Controlled Membrane Mechanics and Shape Transitions of Photoswitchable Lipid Vesicles, *Langmuir* 33(16) (2017) 4083-4089.
- [27] K. Yasuhara, Y. Sasaki, J. Kikuchi, A photo-responsive cholesterol capable of inducing a morphological transformation of the liquid-ordered microdomain in lipid bilayers, *Colloid and Polymer Science* 286(14-15) (2008) 1675-1680.
- [28] P. Urban, S.D. Pritzl, M.F. Ober, C.F. Dirscherl, C. Pernpeintner, D.B. Konrad, J.A. Frank, D. Trauner, B. Nickel, T. Lohmueller, A Lipid Photoswitch Controls Fluidity in Supported Bilayer Membranes, *Langmuir* 36(10) (2020) 2629-2634.
- [29] P. Urban, S.D. Pritzl, D.B. Konrad, J.A. Frank, C. Pernpeintner, C.R. Roeske, D. Trauner, T. Lohmuller, Light-Controlled Lipid Interaction and Membrane Organization in Photolipid Bilayer Vesicles, *Langmuir* 34(44) (2018) 13368-13374.
- [30] J.A. Frank, H.G. Franquelim, P. Schwille, D. Trauner, Optical Control of Lipid Rafts with Photoswitchable Ceramides, *Journal of the American Chemical Society* 138(39) (2016) 12981-12986.
- [31] V.N. Georgiev, A. Grafmuller, D. Bleger, S. Hecht, S. Kunstmann, S. Barbirz, R. Lipowsky, R. Dimova, Area Increase and Budding in Giant Vesicles Triggered by Light: Behind the Scene, *Advanced Science* 5(8) (2018).
- [32] A. Diguët, M. Yanagisawa, Y.-J. Liu, E. Brun, S. Abadie, S. Rudiuk, D. Baigl, UV-Induced Bursting of Cell-Sized Multicomponent Lipid Vesicles in a Photosensitive Surfactant Solution, *Journal of the American Chemical Society* 134(10) (2012) 4898-4904.
- [33] Y. Suzuki, K.H. Nagai, A. Zinchenko, T. Hamada, Photoinduced Fusion of Lipid Bilayer Membranes, *Langmuir* 33(10) (2017) 2671-2676.
- [34] S.H. Donaldson, Jr., C.T. Lee, Jr., B.F. Chmelka, J.N. Israelachvili, General hydrophobic interaction potential for surfactant/lipid bilayers from direct force measurements between light-modulated bilayers, *Proceedings of the National Academy of Sciences of the United States of America* 108(38) (2011) 15699-15704.
- [35] T. Narayanan, H. Wacklin, O. Konovalov, R. Lund, Recent applications of synchrotron radiation and neutrons in the study of soft matter, *Crystallography Reviews* 23(3) (2017) 160-226.
- [36] R. Lund, L. Willner, D. Richter, Kinetics of Block Copolymer Micelles Studied by Small-Angle Scattering Methods, in: A. Abe, K.-S. Lee, L. Leibler, S. Kobayashi (Eds.), *Controlled Polymerization and Polymeric Structures: Flow Microreactor Polymerization, Micelles Kinetics, Polypeptide Ordering, Light Emitting Nanostructures*, Springer International Publishing, Cham, 2013, pp. 51-158.
- [37] G.V. Jensen, R. Lund, T. Narayanan, J.S. Pedersen, Transformation from Globular to Cylindrical Mixed Micelles through Molecular Exchange that Induces Micelle Fusion, *The Journal of Physical Chemistry Letters* 7(11) (2016) 2039-2043.
- [38] G.V. Jensen, R. Lund, J. Gummel, T. Narayanan, J.S. Pedersen, Monitoring the Transition from Spherical to Polymer-like Surfactant Micelles Using Small-Angle X-Ray Scattering, *Angewandte Chemie International Edition* 53(43) (2014) 11524-11528.
- [39] G.V. Jensen, R. Lund, J. Gummel, M. Monkenbusch, T. Narayanan, J.S. Pedersen, Direct Observation of the Formation of Surfactant Micelles under Nonisothermal Conditions by Synchrotron SAXS, *Journal of the American Chemical Society* 135(19) (2013) 7214-7222.
- [40] M. Gradzielski, Kinetics of morphological changes in surfactant systems, *Current Opinion in Colloid & Interface Science* 8(4-5) (2003) 337-345.
- [41] M. Cocera, O. Lopez, R. Pons, H. Amenitsch, A. de la Maza, Effect of the electrostatic charge on the mechanism inducing liposome solubilization: A kinetic study by synchrotron radiation SAXS, *Langmuir* 20(8) (2004) 3074-3079.
- [42] J. Gummel, M. Sztucki, T. Narayanan, M. Gradzielski, Concentration dependent pathways in spontaneous self-assembly of unilamellar vesicles, *Soft Matter* 7(12) (2011) 5731-5738.
- [43] T.M. Weiss, T. Narayanan, M. Gradzielski, Dynamics of spontaneous vesicle formation in fluorocarbon and hydrocarbon surfactant mixtures, *Langmuir* 24(8) (2008) 3759-3766.
- [44] T. Narayanan, M. Sztucki, P. Van Vaerenbergh, J. Leonardon, J. Gorini, L. Claustre, F. Sever, J. Morse, P. Boesecke, A multipurpose instrument for time-resolved ultra-small-angle and coherent X-ray scattering, *Journal of Applied Crystallography* 51(6) (2018) 1511-1524.
- [45] E. Sutherland, S.M. Mercer, M. Everist, D.G. Leaist, Diffusion in Solutions of Micelles. What Does Dynamic Light Scattering Measure?, *Journal of Chemical & Engineering Data* 54(2) (2009) 272-278.
- [46] M. le Maire, P. Champeil, J.V. Möller, Interaction of membrane proteins and lipids with solubilizing detergents, *Biochimica et Biophysica Acta (BBA) - Biomembranes* 1508(1) (2000) 86-111.
- [47] M. Almgren, Mixed micelles and other structures in the solubilization of bilayer lipid membranes by surfactants, *Biochimica Et Biophysica Acta-Biomembranes* 1508(1-2) (2000) 146-163.

- [48] R.F. Correia, M.I. Viseu, T.J.V. Prazeres, J.M.G. Martinho, Spontaneous vesicles, disks, threadlike and spherical micelles found in the solubilization of DMPC liposomes by the detergent DTAC, *Journal of Colloid and Interface Science* 379 (2012) 56-63.
- [49] J. Gustafsson, G. Orädd, M. Nyden, P. Hansson, M. Almgren, Defective Lamellar Phases and Micellar Polymorphism in Mixtures of Glycerol Monooleate and Cetyltrimethylammonium Bromide in Aqueous Solution, *Langmuir* 14(18) (1998) 4987-4996.
- [50] B. Carion-Taravella, J. Chopineau, M. Ollivon, S. Lesieur, Phase Behavior of Mixed Aqueous Dispersions of DPPC and Dodecyl Glycosides: Aggregation States Implicated in the Micelle-to-Vesicle Transition, *Langmuir* 14(14) (1998) 3767-3777.
- [51] P.R. Majhi, A. Blume, Temperature-induced micelle-vesicle transitions in DMPC-SDS and DMPC-DTAB mixtures studied by calorimetry and dynamic light scattering, *Journal of Physical Chemistry B* 106(41) (2002) 10753-10763.
- [52] H. Heerklotz, Interactions of surfactants with lipid membranes, *Quarterly Reviews of Biophysics* 41(3-4) (2008) 205-264.
- [53] C.T. Lee, Jr., K.A. Smith, T.A. Hatton, Small-Angle Neutron Scattering Study of the Micellization of Photosensitive Surfactants in Solution and in the Presence of a Hydrophobically Modified Polyelectrolyte, *Langmuir* 25(24) (2009) 13784-13794.
- [54] C. Herdes, E.E. Santiso, C. James, J. Eastoe, E.A. Mueller, Modelling the interfacial behaviour of dilute light-switching surfactant solutions, *Journal of Colloid and Interface Science* 445 (2015) 16-23.
- [55] T.G. Shang, K.A. Smith, T.A. Hatton, Photoresponsive surfactants exhibiting unusually large, reversible surface tension changes under varying illumination conditions, *Langmuir* 19(26) (2003) 10764-10773.
- [56] C. Blayo, J.E. Houston, S.M. King, R.C. Evans, Unlocking Structure-Self-Assembly Relationships in Cationic Azobenzene Photosurfactants, *Langmuir* 34(34) (2018) 10123-10134.